Hindawi
Mathematical Problems in Engineering
Volume 2018, Article ID 3489082, 13 pages
https://doi.org/10.1155/2018/3489082

Research Article

A Research on Fatigue Damage Constitutive Equation of Asphalt Mixture

Yazhen Sun,[1] **Chenze Fang**,[1] **Dong Fan**,[1] **Jinchang Wang**,[2] **and Xuezhong Yuan**[1]

[1]*Shenyang Jianzhu University, Shenyang, China*
[2]*Institute of Transportation Engineering, Zhejiang University, Hangzhou, China*

Correspondence should be addressed to Jinchang Wang; wjc501@zju.edu.cn

Received 18 April 2018; Accepted 10 June 2018; Published 25 July 2018

Academic Editor: Manuel Pastor

The laboratory investigations of fatigue damage constitutive equation of asphalt mixture were carried out by three-point bending fatigue tests. The three-point bending fatigue tests were performed at three levels of stress-strength ratio (SSR), temperature, and loading rate. The coupled multifactor (stress-strength ratio, temperature, and loading rate) fatigue life equation was established, which can well predict the fatigue life of the asphalt mixture. Both a damage model and a damage evolution equation have been established based on the *E-N* curve, which indicate that fatigue damage evolution is nonlinear and consists of three stages. The sensitivity analysis of damage model parameters indicates that each parameter has different effects on the three stages of damage evolution. Based on the researches above, the fatigue damage constitutive equations were finally built based on the σ-ε curves, which consist of two parts: the damage accumulation stage and the fatigue failure stage. The elasticity-power hardening model was used to describe the constitutive relation of damage accumulation stage. The elasticity-power hardening model and the *Sidoroff* damage model were used to describe the constitutive relation of damage failure stage. The constitutive equations can well characterize the fatigue damage performance of the asphalt mixtures under cyclic loading.

1. Introduction

In recent years, the road construction industry has made great progress with the rapid development of economy, but the quality of the existing roads is uneven. The asphalt concrete pavement, as the surface course of the road structure, is exposed completely to the environment, receiving repeated actions of vehicle loads and environment influence by seasonal changes. The internal stresses and strains of the material change continuously, resulting in the degradation of strength under repetitive load cycles. The pavement under a cumulative load is prone to fatigue failure. The fatigue behaviors of pavement materials have become the research directions of an increasing number of researchers [1–4].

In order to describe the damage evolution and stress-strain relationship of asphalt mixture, many damage models have been proposed [1, 2, 5], such as *Loland* damage model, *Sidoroff* damage model, *Mazars* damage model, and *ExpAsso* damage model. The *Loland* damage model indicates that the stress-strain relationship of material is linear after reaching the peak stress, which is an approximate version [6]. The constitutive equation corresponding to *Sidoroff* damage model, obtained based on the energy equivalence assumption, indicates that the stress-strain relationship of material is linear before reaching the peak stress, which is an approximate version [7]. The *Mazars* damage model indicates that material is not damaged before reaching the peak stress, which is an approximate version [8]. The *ExpAsso* damage model consisted of four parameters indicating that fatigue damage evolution is nonlinear and consists of three stages [9]. However, the physical meanings of model parameters have not been analyzed.

Although the above researches are a big step towards the goal of describing damage evolution and constitutive equation asphalt mixture, there are concerns associated with these researches. The above models only studied the constitutive equations of materials under a single load and did not study the constitutive equations of materials subjected to cyclic loading. However, asphalt pavement is subjected to vehicle cyclic loading, and the researches on the fatigue

Figure 1: Rut board forming machine.

Figure 2: Specimen beams.

Figure 3: Laboratory fatigue test.

damage constitutive equation of asphalt mixture under cyclic loading are rarely found.

To describe the stress-strain relationship of asphalt mixtures under cyclic loading more intuitively and accurately, it is necessary to obtain a simplified and specific constitutive equation. Due to the discontinuity and nonuniformity of the asphalt mixture at the micro level, the constitutive relationship of the asphalt mixture in a fatigue test is more complicated. The constitutive equation and damage evolution of each damage model also differ widely. It is not appropriate to describe the constitutive equations only by using elastic or plastic theory, nor is it to describe the fatigue damage constitutive equation by applying only one existing damage model directly [4, 10, 11].

Laboratory fatigue tests have been carried out to solve the problems above. The influence of experimental factors on test results is studied to obtain the coupled multifactor fatigue life equation. Both a damage model and a damage evolution equation have been established based on the *E-N* curve. The sensitivity analysis of damage model parameters was used to study the physical meanings of model parameters. Based on the researches above, the fatigue damage constitutive equations were finally built based on the σ-ε curves, which consists of two parts: the damage accumulation stage and fatigue failure stage.

2. Establishment of Fatigue Equation

2.1. Test Design

2.1.1. Test Materials. Bitumen penetration grade 70 was used as asphalt binder for preparations of the specimens, with its specifications listed in Table 1. The aggregate gradation type is AC-13, as listed in Table 2.

2.1.2. Preparation of Specimen. A rut board of 400 mm × 400 mm × 70 mm was performed by using a hydraulic sample forming machine, presented in Figure 1. By cutting the rut board, the specimen beams of 250 mm × 30 mm × 35 mm were obtained, and it is presented in Figure 2.

2.1.3. Test Conditions and Methods. The laboratory fatigue test is presented in Figure 3. The flexural tensile strengths of specimens under different test conditions were measured. The specimens were tested using three stress-strength ratios: 0.3, 0.4, and 0.5; three temperatures: 5, 15, and 25°C; and three loading rates: 5, 10, and 20 mm/min.

Table 1: Properties of asphalt rubber.

Material property	Used standard	Value
Softening point	T0606—2000	57 (°C)
Viscosity	T0625—2000	1.5-4.0 (Pa·s)
Elastic recovery	T0662—2000	30 (%)

Table 2: Aggregate gradation.

Sieve size (mm)	16.0	13.2	9.5	4.75	2.36	1.18	0.6	0.3	0.15	0.075
Passing percentage	100.0	91.1	80.2	54.0	33.2	22.5	16.0	12.1	8.7	5.5

2.2. Test Results. The fatigue test was carried out according to the test scheme, and the fatigue lives are listed in Table 3, from which it can be seen that there is a negative correlation between the fatigue life and the stress-strength ratio and loading rate and a positive correlation between the fatigue life and the temperature.

2.3. The Influence of Experimental Factors on Test Results. The fatigue failure of the beam specimen is mainly caused by the tensile stress at the bottom of the specimen, because the ultimate tensile stress of asphalt mixture is far weaker than its ultimate compressive stress. When the cyclic load below the ultimate bending resistance is applied to the beam specimen, the fatigue failure of the beam specimen occurs because of the stress concentration at the bottom, and the fatigue damage is mainly manifested by fatigue cracks. The growth process of a fatigue crack consisted of two stages: the crack initiation and crack propagation. Damage gradually accumulates with the increase of load number. Fatigue cracks occur at the bottom of the beam specimen when the damage is accumulated to a certain extent. Fatigue cracks will expand due to the increase of load number. The cumulative result of the expansion is the fracture of beam specimen [12–14].

2.3.1. The Influence of Stress-Strength Ratio on Fatigue Test. The fatigue lives under the stress-strength ratio of 0.3, 0.4, and 0.5, respectively, are presented in Table 3. It can be seen from Table 3 that there is a negative correlation between the fatigue life and the stress level. The larger the stress-strength ratio is and the greater the load is applied, the greater the accumulation of damage is after each cycle of loading and the shorter the fatigue life becomes [15].

Linear fitting for the logarithmic fatigue life measured under the stress-strength ratio of 0.3, 0.4, and 0.5, respectively, was carried out, and the results are presented in Figure 4. The curve equations of fatigue life are listed in Table 4.

It can be seen from Figure 4 and Table 4 that the logarithmic fatigue life decreases with the increase of stress-strength ratio. A linear function can well describe the relation of logarithmic fatigue life to stress-strength ratio, which can be expressed as

$$\lg N_f = a - b\mathrm{SSR} \tag{1}$$

where $\lg N_f$ is the logarithmic fatigue life, SSR is the stress-strength ratio, and a and b are constants.

2.3.2. The Influence of Temperature on Fatigue Test. The fatigue lives at temperature of 5, 15, and 25°C, respectively, are presented in Figure 5. As shown in the figure, there is a positive correlation between the fatigue life and the temperature. Asphalt mixture is a viscoelastic material. The healing of asphalt mixtures improves with the increase of temperature. In the meantime, the corresponding fatigue life increases [16–18].

2.3.3. The Influence of Loading Rate on Fatigue Test. The fatigue lives under the loading rate of 5 mm/min, 10 mm/min, and 20 mm/min, respectively, are presented in Figure 6. As shown in the figure, there is a negative correlation between the fatigue life and the loading rate. The mechanical behavior of asphalt mixture under dynamic load is different from that under static load. In addition to the magnitude of the load, the mechanical behavior is also related to the loading rate and the deformation rate of the material. When a cyclic loading was applied to the beam specimen, the deformation rate increased with the increase of the loading rate. After each loading cycle, the healing of asphalt mixtures is not fully exploited, which leads to a rise in the rate of damage accumulation and a decline in fatigue life [12, 18–20].

2.4. Construction of Coupled Multifactor Fatigue Equation. Based on the analysis above, it is obvious that the fatigue life is related to stress-strength ratio, temperature, and loading rate. In order to accurately describe the relationship between fatigue life and experimental factors, linear regressions were made in the three experimental factors. A linear function can well describe the relation of logarithmic fatigue life to the three experimental factors, which can be expressed as

$$\begin{aligned} \lg N_f &= 4.26838 + 0.02355T - 3.64776\mathrm{SSR} \\ &\quad - 0.01619V, \\ R^2 &= 0.99374 \end{aligned} \tag{2}$$

where $\lg N_f$ is the logarithmic fatigue life, T is the temperature, SSR is the stress-strength ratio, and V is the loading rate.

Equation (2) is a fatigue equation that couples the stress-strength ratio, the temperature, and the loading rate.

Table 3: The fatigue life.

Loading rate (V) / mm / min	Stress-strength ratio (SSR)	Value (N_f)		
		5°C	15°C	25°C
5	0.3	1,586	2,770	4,842
	0.4	631	1,413	2,000
	0.5	324	490	920
10	0.3	1,324	2,313	4,044
	0.4	617	1,122	1,585
	0.5	229	407	776
20	0.3	924	1,613	2,820
	0.4	432	631	1,096
	0.5	175	303	537

Table 4: Linear regression results.

Temperature (T) / °C	Loading rate (V) / mm / min		
	5	10	20
5	$\lg N_f$=4.21-3.45SSR, R^2=0.98312	$\lg N_f$=4.28-3.80SSR, R^2=0.98901	$\lg N_f$=4.06-3.61SSR, R^2=0.99507
15	$\lg N_f$=4.59-3.76SSR, R^2=0.96751	$\lg N_f$=4.51-3.77SSR, R^2=0.98162	$\lg N_f$=4.28-3.62SSR, R^2=0.98989
25	$\lg N_f$=4.75-3.60SSR, R^2=0.96643	$\lg N_f$=4.66-3.58SSR, R^2=0.96643	$\lg N_f$=4.51-3.60SSR, R^2=0.96643

2.5. The Analysis of the Fatigue Equation. The load magnitude applied to the asphalt mixture is reflected by the stress-strength ratio of fatigue tests and the axle load of asphalt pavements. The specimen subjected to a larger stress-strength ratio, which corresponds to a larger axle load that a pavement is subjected to, has a shorter fatigue life.

The number of vehicle loads in a specific time is reflected by the loading rate of fatigue tests and the traffic volume of asphalt pavements. The specimen subjected to a larger loading rate, which corresponds to a larger traffic volume that a pavement is subjected to, has a shorter fatigue life.

It can be seen from the qualitative analysis that the coupled multifactor fatigue equation can well characterize the influence of the vehicle load and traffic volume on the fatigue life of asphalt pavements.

3. Construction of Damage Evolution Equation

3.1. Construction of Damage Evolution Equation. The stress-strain relation of damaged specimens during fatigue test is described on the basis of strain equivalence and damage mechanics, i.e.,

$$E = \frac{E_0}{(1 - D)} \tag{3}$$

$$D = 1 - \frac{E}{E_0} \tag{4}$$

where E_0 is the initial modulus, E is the modulus during fatigue loading, and D is the damage factor.

The E-N curve is shown in Figure 7. As shown in the figure, the modulus decreases with the increase of the number of loading cycles. The E/E_0-N/N_f curve was obtained by dividing the abscissa and the ordinate of E-N curve by E_0 and N_f, respectively. The E/E_0-N/N_f curve is shown in Figure 8. It can be seen that the process can be divided into three stages. In the first stage, the modulus decreases sharply and fatigue cracks emerge. In the second stage, the modulus decreases stably and fatigue cracks expand. In the third stage, the modulus decreases rapidly and the beam fractures finally. The cumulative result of the expansion was the fracture of the beam specimen. The following equation was used to fit the E/E_0-N/N_f curve:

$$\frac{E}{E_0} = 1 - \sum_{i=1}^{2} A_i \left(1 - e^{-(N/N_f)/K_i}\right) \tag{5}$$

where A_i and K_i are model parameters, N is the number of loading cycles, and N_f is the fatigue life.

The model parameters are obtained by fitting the experimental data. As listed in Table 5, the squared correlation coefficients (R^2) are over 0.99. As can be seen from Table 5, the fitting parameters are related to the experimental factors, such as the temperature, the loading rate, and the stress-strength ratio. A quadratic polynomial is used to fit the experimental data. The regression results are as follows.

$A_1 = 0.685 - 0.0282\ T + 0.00106\ T^2 + 0.00474 \times 10^{12}\ V - 5.364 \times 10^{-4}\ V^2 - 0.0157\ \mathrm{SSR} - 0.825\ \mathrm{SSR}^2$, $R^2 = 0.874$.

$K_1 = -0.00976 + 0.00286\ T - 1.673 \times 10^{-4}\ T^2 + 0.00292 \times 10^{11}\ V - 5.528 \times 10^{-5}\ V^2 - 0.0201\ \mathrm{SSR} + 0.35628\ \mathrm{SSR}^2$, $R^2 = 0.82995$.

$A_2 = 1.330 + 0.0355\ T - 0.00210\ T^2 - 0.0347\ V + 0.00205\ V^2 - 4.924\ \mathrm{SSR} + 8.983\ \mathrm{SSR}^2$, $R^2 = 0.757$.

$K_2 = 2.628 + 0.0413\ T - 0.00364\ T^2 + 0.0735\ V - 0.00152\ V^2 - 13.579\ \mathrm{SSR} + 23.267\ \mathrm{SSR}^2$, $R^2 = 0.614$.

The damage model function is expressed as

$$D = 1 - \frac{E_i}{E_0} = \sum_{i=1}^{2} A_i \left(1 - e^{-(N/N_f)/K_i}\right) \tag{6}$$

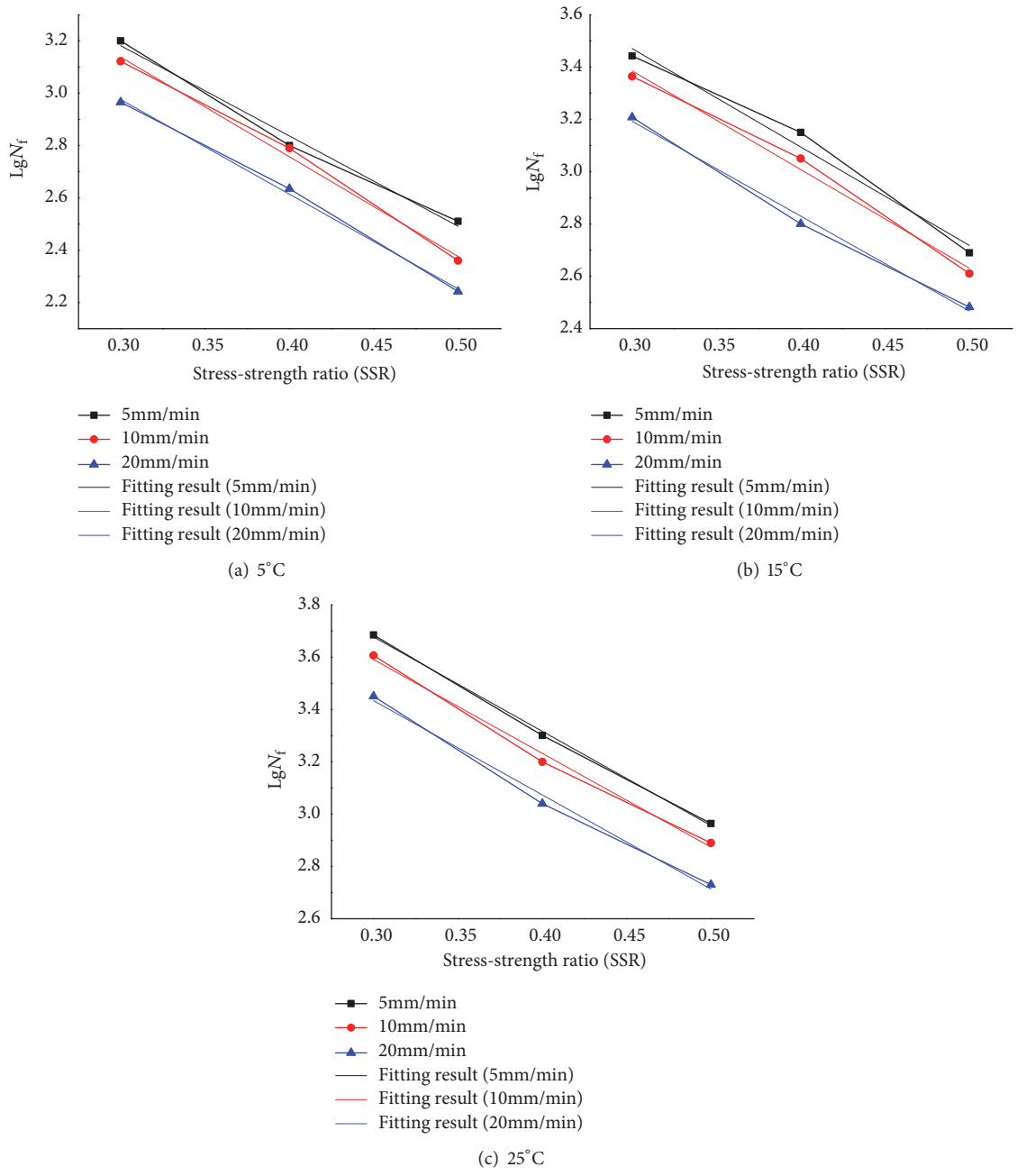

FIGURE 4: The logarithmic fatigue lives at different stress-strength ratios.

Damage evolution equation is obtained by calculating the derivative of (6), and the damage evolution equation is expressed as

$$\frac{dD}{dN} = \sum_{i=1}^{2} A_i e^{-(N/N_f)/K_i} \frac{1}{K_i N_f} \tag{7}$$

The D-N/N_f curve is shown in Figure 9. As presented in the figure, the damage increases nonlinearly during the fatigue tests, and the process can be divided into three stages, which is similar to the process of degradation of modulus. In the first stage, the damage lasts a short time but increases rapidly, and, in the end of this stage, it reaches a large value. In the second stage, the damage lasts a long time and increases stably. In the third stage, the damage increases sharply and the beam fractures finally [9].

3.2. Sensitivity Analysis of Damage Model Parameters. As shown in Table 5, the value ranges of A_1, K_1, A_2, and K_2 are 0.110-0.554, 0.013-0.122, 0.269-1.134, and 0.118-1.878, respectively. Three data sets are taken within the range of each parameter and are listed in Table 6. The influences of the four parameters (A_1, K_1, A_2, K_2) on the three stages of damage evolution are analyzed.

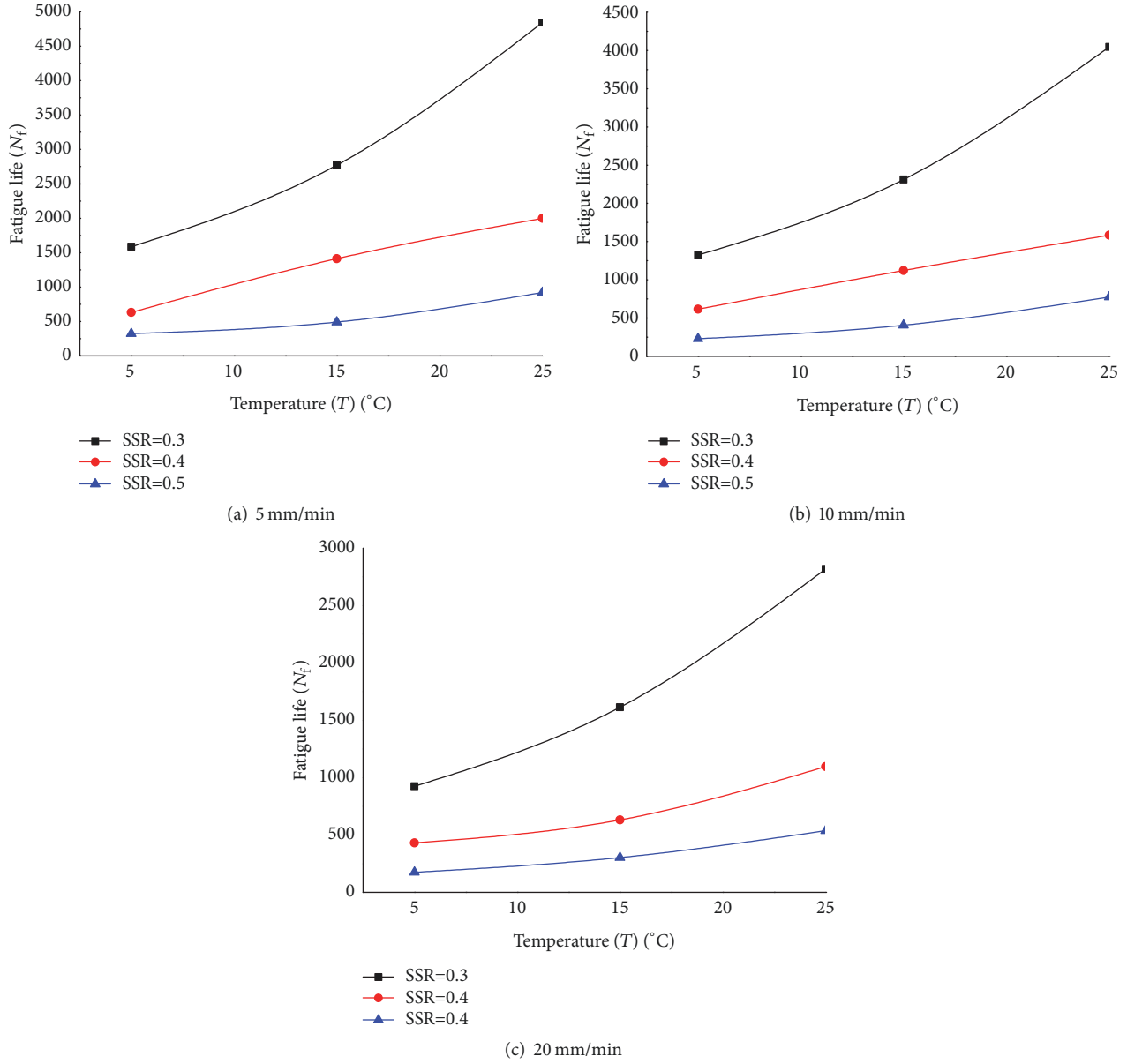

Figure 5: Fatigue lives at different temperatures.

3.2.1. Analysis of Parameter A_1. Set the values for parameter A_1 as 0.1, 0.3, and 0.5, respectively, and other parameters keep invariant; the D-N/N_f curves are plotted in Figure 10. As shown in the figure, the three stages of damage evolution are greatly influenced by parameter A_1. The larger parameter A_1 is, the more serious the degree of the damage of material becomes. Parameter A_1 is a main parameter that influences the degree of the damage of material.

3.2.2. Sensitivity Analysis of Parameter K_1. Set the values for parameter K_1 as 0.04, 0.08, and 0.12, respectively, and other parameters keep invariant; the D-N/N_f curves are plotted in Figure 11. As shown in the figure, as the parameter K_1 changes, the second and third stages of damage evolution are less influenced, but the first stage is greatly influenced. The larger parameter K_1 is, the longer the duration of the first stage lasts. Parameter K_1 is a parameter that influences the rate of the damage evolution in the first stage.

3.2.3. Sensitivity Analysis of Parameter A_2. Set the values for parameter A_2 as 0.2, 0.4, and 0.6, respectively, and other parameters keep invariant; the D-N/N_f curves are plotted in Figure 12. As shown in the figure, as parameter A_2 changes, the first stage of damage evolution is less influenced, but the second and third stages are greatly influenced. The larger parameter A_2 is, the faster the rate of damage evolution is, and the more serious the degree of the damage of material becomes in the second and third stages. Parameter A_2 is a parameter that influences the rate and the degree of the damage evolution in the second and third stages.

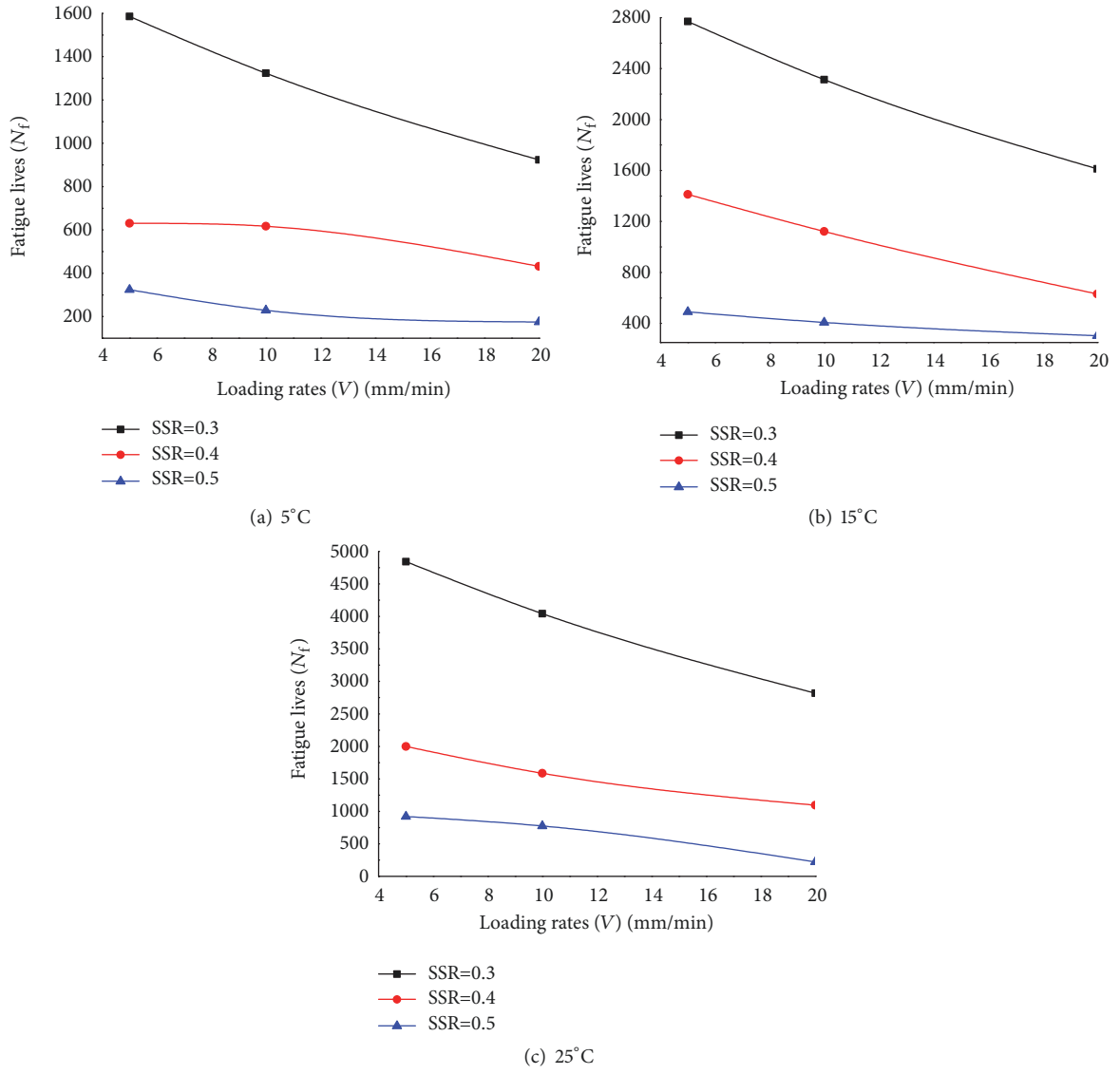

Figure 6: Fatigue lives under different loading rates.

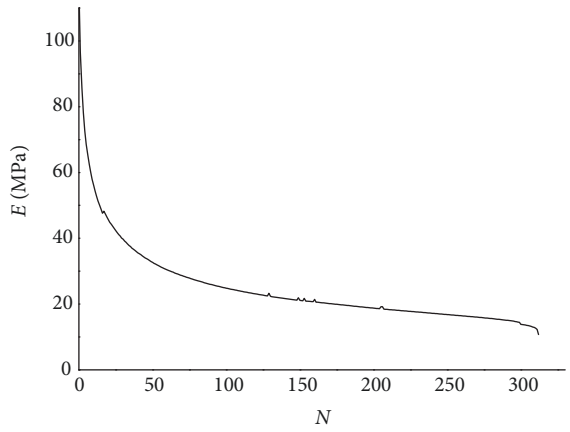

Figure 7: E-N curve.

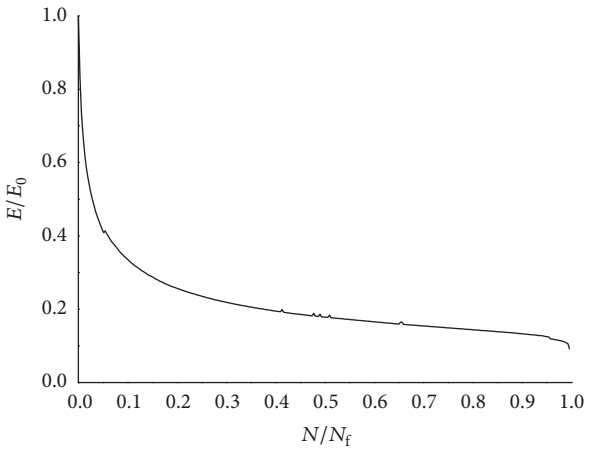

Figure 8: E/E_0-N/N_f curve.

Table 5: Fitting parameters.

Temperature (T) / °C	Loading rate (V) / mm/min	stress-strength ratio (SSR)	A_1	K_1	A_2	K_2
5	5	0.3	0.495	0.034	0.538	0.997
		0.4	0.465	0.072	0.633	1.089
		0.5	0.350	0.094	1.332	1.837
	10	0.3	0.471	0.041	0.511	0.837
		0.4	0.442	0.087	0.601	1.304
		0.5	0.333	0.113	1.271	3.137
	20	0.3	0.434	0.054	1.184	2.588
		0.4	0.308	0.068	1.233	2.360
		0.5	0.192	0.122	1.134	1.878
15	5	0.3	0.422	0.034	0.535	0.502
		0.4	0.350	0.053	0.648	0.729
		0.5	0.302	0.096	1.253	2.546
	10	0.3	0.419	0.044	0.520	0.710
		0.4	0.332	0.063	0.615	0.875
		0.5	0.287	0.115	1.190	3.055
	20	0.3	0.308	0.043	0.605	0.888
		0.4	0.320	0.080	1.221	2.200
		0.5	0.109	0.112	1.276	1.677
25	5	0.3	0.554	0.013	0.269	0.117
		0.4	0.499	0.017	0.307	0.228
		0.5	0.485	0.025	0.401	0.598
	10	0.3	0.527	0.016	0.283	0.161
		0.4	0.486	0.022	0.327	0.298
		0.5	0.477	0.032	0.421	0.546
	20	0.3	0.435	0.032	0.393	0.365
		0.4	0.329	0.057	0.482	0.518
		0.5	0.315	0.081	0.635	0.953

Table 6: The parameter values.

Parameter	A_1	K_1	A_2	K_2
Value	0.1,0.3,0.5	0.04,0.08,0.12	0.2,0.4,0.6	0.1,0.6,1.1

3.2.4. Sensitivity Analysis of Parameter K_2. Set the values for parameter K_2 as 0.1, 0.6, and 1.1, respectively, and other parameters keep invariant; the D-N/N_f curves are plotted in Figure 13. As shown in the figure, as parameter K_2 changes, the first stage of damage evolution is less influenced, but the second and third stages are greatly influenced. The larger parameter K_2 is, the slower the rate of damage evolution is, and the less serious the degree of the damage of material becomes in the second and third stages. Parameter K_2 is a parameter that influences the rate and degree of the damage evolution in the second and third stages.

3.2.5. Result of the Sensitivity Analysis. Parameter A_1 is a main parameter that influences the degree of the damage of material. Parameter K_1 is a parameter that influences the speed of the damage evolution in the first stage. Parameters A_2 and K_2 are parameters that influence the speed and degree of the damage evolution in the second and third stages. A conclusion can be drawn that each parameter has different effects on the three stages of damage evolution.

4. Construction of Fatigue Damage Constitutive Equations

The stress-strain curves were obtained by calculating the fatigue test data. The stress-strain curves of the last five cyclic loadings were chosen in order to clearly draw the stress-strain curves, which are presented in Figure 14. The residual strain increased with the increase of the number of cyclic loadings. Plastic deformation occurred when the damage was

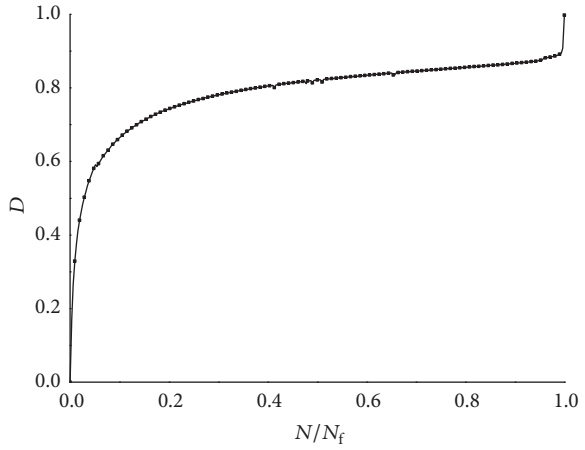

FIGURE 9: D-N/N_f curve.

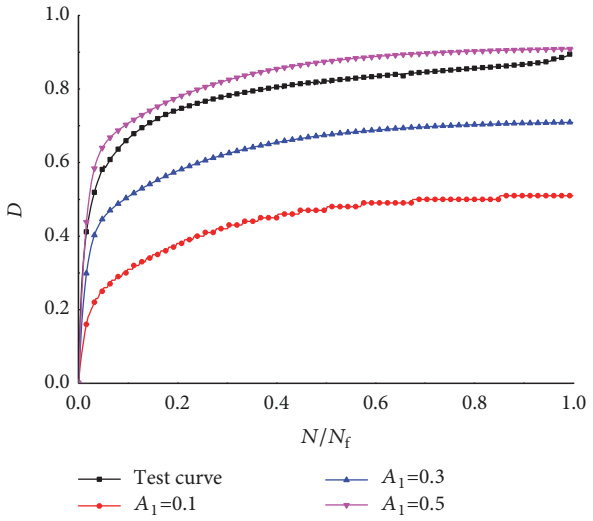

FIGURE 10: D-N/N_f curves (A_1=0.1, 0.3, and 0.5).

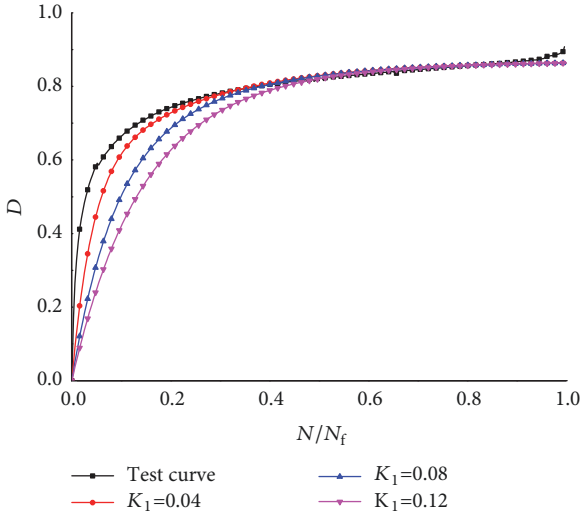

FIGURE 11: D-N/N_f curves (K_1=0.04, 0.08, and 0.12).

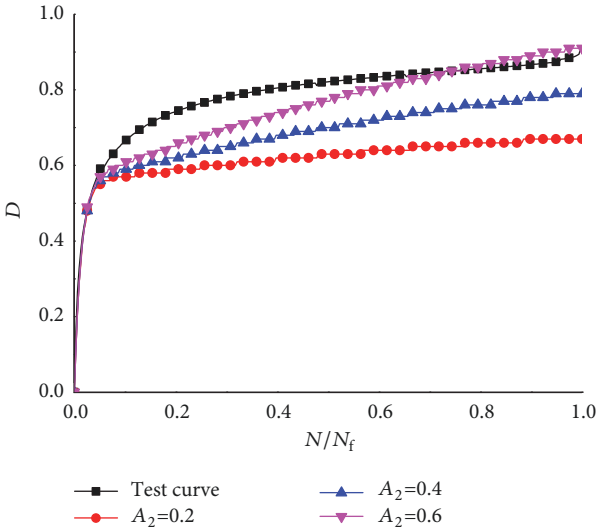

FIGURE 12: D-N/N_f curves (A_2=0.2, 0.4, and 0.6).

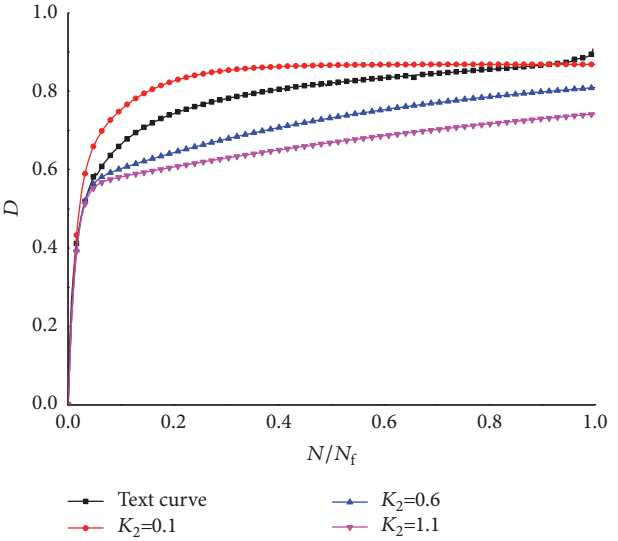

FIGURE 13: D-N/N_f curves (K_2=0.1, 0.6, and 1.1).

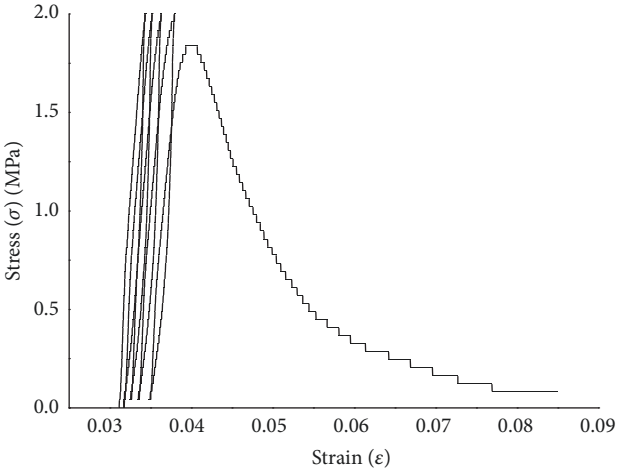

FIGURE 14: Stress-strain curves.

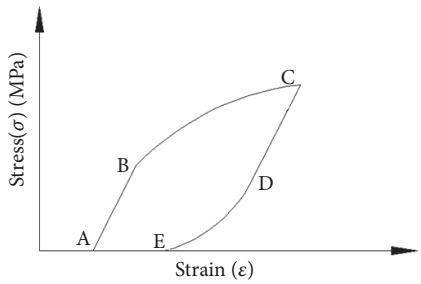

Figure 15: Stress-strain curves of damage accumulation.

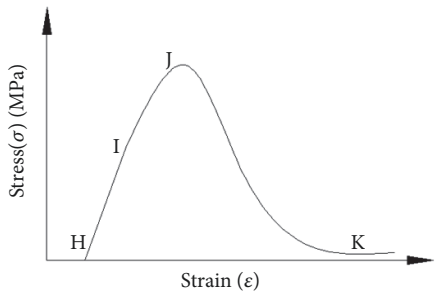

Figure 16: Stress-strain curves of fatigue destruction.

accumulated, and the plastic deformation would influence the damage accumulation. Plastic deformation and damage accumulation are interrelated [9, 21, 22].

Constitutive equation under cyclic loading consists of two parts: one for the damage accumulation stage and the other for the fatigue failure stage. The constitutive equations for the damage accumulation stage before the last cyclic loading are in the same form, and the stress-strain curves are presented in Figure 15. As shown in the figure, the stress-strain curves of damage accumulation stage consist of four parts. The form of the constitutive equations of the last cyclic loading, which is called the damage failure stage, is different from the form for the damage accumulation stage. The stress-strain curves are presented in Figure 16. As shown in the figure, the stress-strain curves of damage accumulation stage consist of three parts.

4.1. Construction of Constitutive Equations of the Damage Accumulation Stage. The elasticity-power hardening model can be used to describe the stress-strain relationship of the material [21] and is expressed as

$$\sigma = \begin{cases} E\varepsilon, & 0 \le \sigma \le \sigma_0 \\ k\varepsilon^n, & \sigma > \sigma_0 \end{cases} \tag{8}$$

where σ is the stress, ε is the strain, E is the elastic modulus, and k and n are material constants obtained by fitting the test data.

The elasticity-power hardening model, a widely used mechanical model, can not only well describe the plastic deformation of the material, but also can well describe the elastic deformation of the material [21].

Figure 15 shows that constitutive relation of the loading stage consisted of two parts. The material in part AB is elastic, and the material in part BC is elastic-plastic. The asphalt mixture in the part AB has the characteristics of linear deformation; the asphalt mixture in part BC has the characteristic of nonlinear deformation. Therefore, the elasticity-power hardening model was used to describe the constitutive relation of damage accumulation stage in the loading stage. Constitutive relation of the unloading stage consisted of two parts. The asphalt mixture in the part CD has the characteristics of linear deformation. The asphalt mixture in the part DE has the characteristics of nonlinear deformation. The elasticity-power hardening model indicates that linear function can well describe the elastic deformation of the material, and the power function can well describe the elastic-plastic deformation of the material. Therefore, the elasticity-power hardening model was used to describe the constitutive relation of damage accumulation stage in the unloading stage. In this paper, the constitutive equations for the elastic and the elastic-plastic state are expressed by the linear function and the power function, respectively [9, 21, 23].

The constitutive equations for the damage accumulation state are expressed as follows.

Loading stage is

$$\sigma = \begin{cases} E_0 (1-D)\,\varepsilon^* = E_0 \left[1 - \sum_{i=1}^{2} A_i \left(1 - e^{-(N/N_f)/K_i}\right)\right] \varepsilon^*, & \varepsilon_A \le \varepsilon < \varepsilon_B \\ (1-D)\,a_1 \left(\varepsilon^* - a_2\right)^{a_3} = \left[1 - \sum_{i=1}^{2} A_i \left(1 - e^{-(N/N_f)/K_i}\right)\right] a_1 \left(\varepsilon^* - a_2\right)^{a_3}, & \varepsilon_B \le \varepsilon < \varepsilon_C \end{cases} \tag{9}$$

Unloading stage is

$$\sigma = \begin{cases} E_0 (1-D)\,\varepsilon^{**} = E_0 \left[1 - \sum_{i=1}^{2} A_i \left(1 - e^{-(N/N_f)/K_i}\right)\right] \varepsilon^{**}, & \varepsilon_C \le \varepsilon < \varepsilon_D \\ (1-D)\,a_4 \left(\varepsilon^{***} + 1\right)^{a_5} = \left[1 - \sum_{i=1}^{2} A_i \left(1 - e^{-(N/N_f)/K_i}\right)\right] a_4 \left(\varepsilon^{***} + 1\right)^{a_5}, & \varepsilon_D \le \varepsilon \le \varepsilon_E \end{cases} \tag{10}$$

Table 7: Fitting results for damage accumulation.

Fitting parameters	a_1	a_2	a_3	a_4	a_5
Value	146.20	-3.01×10^{-4}	0.79	0.12	1658.19

where ε_A, ε_B, ε_C, ε_D, and ε_E are the stains at points A, B, C, D, and E, respectively, $\varepsilon^* = \varepsilon - \varepsilon_A$, $\varepsilon^{**} = \varepsilon - \varepsilon_B$, $\varepsilon^{***} = \varepsilon - \varepsilon_C$, a_1, a_2, a_3, a_4, and a_5 are fitting parameters.

The properties of asphalt mixture are stable after 30 cycles of loading. The constitutive equation of the 30th loading cycle of the fatigue test at the temperature of 25°C, the stress-strength ratio of 0.4, and the loading rate of 10 mm/min was obtained by fitting the data. The fitting results are listed in Table 7, and the squared correlation coefficient (R^2) is larger than 0.98. The fitting and the test curve are shown in Figure 17. As shown in the figure, the fatigue behavior of the asphalt mixture is well represented by the proposed constitutive equation. Because the characteristics of the constitutive relations before the last cyclic loading are the same, the proposed constitutive equations of the damage accumulation stage are typical.

4.2. Construction of Constitutive Equations of the Damage Failure Stage. The *Sidoroff* damage model can be used to describe the stress-strain relationship of the material [5], and it is expressed as

$$\sigma = \begin{cases} E\varepsilon, & 0 \le \varepsilon \le \varepsilon_f \\ E\varepsilon_f \left(\dfrac{\varepsilon_f}{\varepsilon}\right)^3, & \varepsilon > \varepsilon_f \end{cases} \tag{11}$$

where ε_f is the strain at the peak stress.

Figure 16 shows that the constitutive relation of damage failure stage consists of three parts. The material in part *HI* is elastic, and the material in part *IJ* is elastic-plastic. The constitutive relation of the part *HJ*, similar to the constitutive relation of the part *AC*, is described with the elasticity-power hardening model. The material in part *JK* is elastic-plastic, and the asphalt mixture in the part *JK* has the characteristics of nonlinear deformation. The Sidoroff damage model assumes that damage occurs and cracks are generated when the material reaches its peak stress. The Sidoroff damage model can well describe the nonlinear deformation of the material, so it was used to describe the constitutive relation of the unloading part in the damage failure stage [7, 21, 23].

The constitutive equations of the damage failure stage are expressed as follows:

$$\sigma = \begin{cases} E_0 (1-D)\,\varepsilon' = E_0 \left[1 - \sum_{i=1}^{2} A_i \left(1 - e^{-(N/N_f)/K_i}\right)\right]\varepsilon', & \varepsilon_H \le \varepsilon < \varepsilon_I \\ (1-D)\,b_1 \left(\varepsilon' - b_2\right)^{b_3} = \left[1 - \sum_{i=1}^{2} A_i \left(1 - e^{-(N/N_f)/K_i}\right)\right] b_1 \left(\varepsilon' - b_2\right)^{b_3}, & \varepsilon_I \le \varepsilon < \varepsilon_J \\ b_4 \left(\dfrac{b_5}{\varepsilon' - b_6}\right)^3, & \varepsilon_J \le \varepsilon \le \varepsilon_K \end{cases} \tag{12}$$

where ε_H, ε_I, ε_J, and ε_K are the strains at points H, I, J, and K, respectively, $\varepsilon' = \varepsilon - \varepsilon_H$, $\varepsilon_J{}' = \varepsilon_J - \varepsilon_H$, and b_1, b_2, b_3, b_4, b_5, and b_6 are fitting parameters.

The constitutive equation of the fatigue test at the temperature of 25°C, the stress-strength ratio of 0.3, and the loading rate of 10 mm/min was obtained by fitting the data. The fitting results are listed in Table 8, and the squared correlation coefficient (R^2) is larger than 0.98. The fitting and the test curve are shown in Figure 18. As shown in the figure, the fatigue performances of the asphalt mixture are well represented by the proposed constitutive equation.

5. Conclusions

Laboratory investigations of the fatigue properties of asphalt mixture were conducted by three-point bending fatigue tests. Test results were analyzed to build fatigue damage constitutive equations. With the study above, the following conclusions can be drawn.

(1) Fatigue life decreases with the increase of stress-strength ratio. The linear function can well describe the relationship between logarithmic fatigue life and stress-strength ratio. The healing of the asphalt mixtures improves as temperature increases, and the corresponding fatigue life increases. The rate of the damage accumulation decreases with the increase of loading rate, and the corresponding fatigue life decreases. The above conclusions may provide a theoretical base for the establishing of fatigue life equation for asphalt mixture.

(2) The coupled multifactor (stress-strength ratio, temperature, and loading rate) fatigue life equation has been established, which can well describe the relationship of the logarithmic fatigue life to the stress-strength ratio, the temperature, and the loading rate and predict the fatigue life of the asphalt mixture and provide a theoretical base for the establishing of fatigue damage model.

(3) Both the damage model and the damage evolution equation have been established based on the *E-N* curve,

Table 8: Fitting results for fatigue destruction.

Fitting parameters	b_1	b_2	b_3	b_4	b_5	b_6
Value	13.50	3.09×10^{-4}	0.48	-0.13	-0.45	-0.023

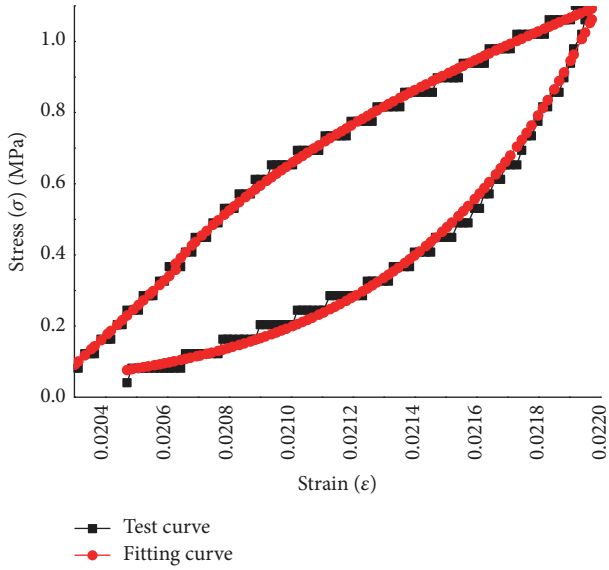

Figure 17: Comparison of σ-ε curve for damage accumulation based on the test and fitting curve.

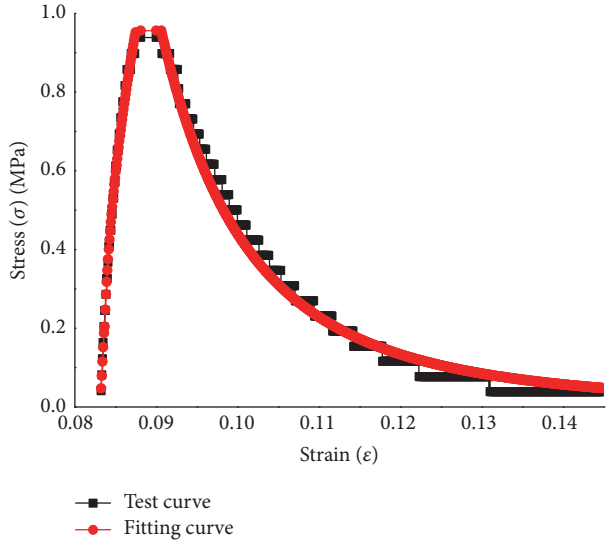

Figure 18: Comparison of σ-ε curve for fatigue destruction based on the test and the fitting curve.

which indicate that fatigue damage evolution is nonlinear and consists of three stages. The sensitivity analysis of damage model parameters indicates that each parameter has different effects on the three stages of damage evolution. The damage model can be used to build the constitutive equations coupling fatigue damage.

(4) The fatigue damage constitutive equations were built based on the σ-ε curves, which consist of two parts: the damage accumulation stage and the fatigue failure stage. The constitutive equation can well characterize the fatigue damage performances of the asphalt mixtures under cyclic loading.

Data Availability

The data used to support the findings of this study are available from the corresponding author upon request.

Conflicts of Interest

The authors declare that there are no conflicts of interest regarding the publication of this paper.

Acknowledgments

This research was performed at the Shenyang Jianzhu University and Institute of Transportation Engineering of Zhejiang University. The research is funded by the National Natural Science Fund (51478276) and the Natural Science Foundation of Liaoning Province (20170540770).

References

[1] R.-X. Xia, J. H. Li, J. He, and D.-F. Shi, "Effect analysis of vehicle system parameters on dynamic response of pavement," *Mathematical Problems in Engineering*, vol. 2015, 8 pages, 2015.

[2] P. Cao, D. Feng, and C. Zhou, "A modified damage-plasticity coupled area-weighted nonlocal model for simulating ductile fracture and softening behaviors of materials," *Mathematical Problems in Engineering*, vol. 2014, 10 pages, 2014.

[3] D. Fei, Y. Yan, C. Liangcai, T. Yaohong, and W. Xuancang, "Mechanical response of typical cement concrete pavements under impact loading," *Mathematical Problems in Engineering*, vol. 2017, 13 pages, 2017.

[4] X. Wang, J. Chen, M. Xiao, and D. Wu, "Seismic response analysis of concrete lining structure in large underground powerhouse," *Mathematical Problems in Engineering*, vol. 2017, 14 pages, 2017.

[5] L. Barba and N. Rodríguez, "Hybrid models based on singular values and autoregressive methods for multistep ahead forecasting of traffic accidents," *Mathematical Problems in Engineering*, vol. 2016, 14 pages, 2016.

[6] K. E. Løland, "Continuous damage model for load-response estimation of concrete," *Cement and Concrete Research*, vol. 10, no. 3, pp. 395–402, 1980.

[7] F. Sidoroff, "Description of anisotropic damage application to elasticity," in *Proceedings of the IUTAM Symposium on Physical no.nlinearites is Structural Mechanics*, Berlin Springer, 1981.

[8] J. Mazars, "A description of micro- and macroscale damage of concrete structures," *Engineering Fracture Mechanics*, vol. 25, no. 5-6, pp. 729–737, 1986.

[9] L. Liqiang and T. Xiaoge, "No.nlinear analysis of fatigue damage of asphalt mixture," *Journal of Building Materia*, vol. 15, no. 4, pp. 508–512, 2012 (Chinese).

[10] D. Sosa, D. Arévalo, E. D. Mora, M. B. Correa, D. Albuja, and C. Gómez, "Experimental and analytical study of slender reinforced concrete shear wall under cyclic in-plane lateral load," *Mathematical Problems in Engineering*, vol. 2017, 14 pages, 2017.

[11] Y. Li, T. J. Mo, S. B. Li, Q. G. Liang, J. P. Li, and R. Qin, "Nonlinear analysis for the crack control of SMA smart concrete beam based on a bidirectional B-spline QR method," *Mathematical Problems in Engineering*, vol. 2018, Article ID 6092479, 16 pages, 2018.

[12] S. C. S. R. Tangella, J. Craus, J. A. Deacon, and C. L. Monismith, "Summary report on fatigue response of asphalt mixtures," *Strategic Highway Research Program Project A-003-A*, 1990.

[13] X. Luo, R. Luo, and R. L. Lytton, "Energy-based mechanistic approach to characterize crack growth of asphalt mixtures," *Journal of Materials in Civil Engineering*, vol. 25, no. 9, pp. 1198–1208, 2013.

[14] Z. Zhang, R. Roque, B. Birgisson, and B. Sangpetgnam, "Identification and verification of a suitable crack growth law for asphalt mixtures," *Journal of the Association of Asphalt Paving Technologists*, vol. 70, pp. 206–241, 2001.

[15] D. Han, B. Zhan, and X. Huang, "Fatigue analysis of the asphalt mixture beam using damage evolution equations," *Advanced Materials Research*, vol. 163-167, pp. 3332–3335, 2011.

[16] B. Ding, *Study on the Fatigue Damage Performance of Asphalt Mixture with considering Loading History*, Chang'an University, Xian, China, 2015.

[17] R. K. Abu Al-Rub, M. K. Darabi, D. N. Little, and E. A. Masad, "A micro-damage healing model that improves prediction of fatigue life in asphalt mixes," *International Journal of Engineering Science*, vol. 48, no. 11, pp. 966–990, 2010.

[18] R. P. Wool and K. M. O'Connor, "A theory of crack healing in polymers," *Journal of Applied Physics*, vol. 52, no. 10, pp. 5953–5963, 1981.

[19] C. Celauro, C. Fecarotti, A. Pirrotta, and A. C. Collop, "Experimental validation of a fractional model for creep/recovery testing of asphalt mixtures," *Construction and Building Materials*, vol. 36, pp. 458–466, 2012.

[20] X. Luo, R. Luo, and R. L. Lytton, "Mechanistic modeling of healing in asphalt mixtures using internal stress," *International Journal of Solids and Structures*, vol. 60, pp. 35–47, 2015.

[21] H. Chen et al., *Elasticity and Plasticity*, Architecture & Building Press, Beijing, China, 2004.

[22] T. Yu, "A segment linear damage model of concrete," *Fracture and Strength of Rock and Concrete*, vol. 2, pp. 14–16, 1982 (Chinese).

[23] E. Masad, L. Tashman, D. Little, and H. Zbib, "Viscoplastic modeling of asphalt mixes with the effects of anisotropy, damage and aggregate characteristics," *Mechanics of Materials*, vol. 37, no. 12, pp. 1242–1256, 2005.